Superimposed Perspective Visual Cues for Helicopter Hovering Above a Moving Ship Deck

M. Negrin,* A. J. Grunwald,† and A. Rosen‡
Technion—Israel Institute of Technology, Haifa, 32000 Israel

The subject of the investigation is a manual low-altitude hovering task above a small moving ship deck using visual field cues supplemented by superimposed display symbology. In this task, rather than tracking the ship-deck motion, the pilot should keep the helicopter inertially stable at a desired inertial position with respect to the ship deck. This hovering stage lasts until the touchdown can be performed during some period of quiescent ship motion. The main difficulties during this task arise from the lack of appropriate visual references necessary to keep the helicopter inertially stable above the ship deck. This research investigates, both analytically and experimentally, the effects of the information superimposed on the visual field on hovering performance. This additional visual information can be implemented by inertial references generated on the ship deck, and/or by a helicopter-based head-up display. For the ship-deck references, inertially stable, three-dimensional visual structures such as line-drawn cubes are investigated. For the head-up display information, only an artificial horizon is investigated. The results of the investigation clearly show that hovering performance is improved by the inclusion of inertially stable visual cues. Moreover, it is shown that the performance is almost independent of the size of the three-dimensional structure. Thus, it is possible to implement the ship-based visual references within practical physical dimensions.

Nomenclature

A = system matrix
B = control matrix
C = observation matrix
h = helicopter vertical displacement, ft
h_s = ship vertical displacement, ft
$\boldsymbol{v}_y(t)$ = observation noise vector with zero-mean Gaussian white noise processes with covariance matrix V
w = helicopter vertical velocity, ft/s
$\boldsymbol{w}_d$ = disturbance vector with covariance matrix W_d
w_g = atmospheric disturbance, ft/s
w_s = ship vertical velocity, ft/s
$\boldsymbol{x}$ = state vector
$\boldsymbol{y}(t)$ = vector of observed variables
δ_c = collective input command, inch lever deflection

I. Introduction

THE manual landing of a helicopter on a small moving ship deck is a very demanding task, particularly in adverse weather and sea conditions. The requirements for both civilian and military helicopter operations from small ships have increased significantly during recent years. As a result, a large number of improvements necessary to meet shipboard operation requirements have been introduced into helicopters. Nevertheless, landing on a ship deck is still performed manually.[1-5] The entire landing procedure can be divided into four main stages: 1) approach to landing, 2) hovering above the landing deck, 3) touchdown, and 4) securing of the helicopter on the deck.

A number of references[6-9] document investigations of the control and information systems for VTOL and helicopter approach to landing (stage 1). The present work concentrates on the second stage, i.e., the hovering above the deck, prior to the touchdown. The required hovering location is referred to as the station keeping point (SKP). Hovering above a moving deck is a much more demanding task than hovering above a fixed location on the ground. It is known that if a pilot attempts to track the ship motion, the ship-to-helicopter distance might become dangerously small, as a result of phase lags between the helicopter and the ship motions. In this case, the pilot must abort the attempt for touchdown and reinitiate the whole procedure. This dangerous and undesired situation can be avoided by hovering at an inertially stable location (SKP) above the moving deck until some moment of quiescent ship motion arrives, during which time the touchdown can be performed.[1] During hovering, the pilot's main source of information originates from the visual field. Since the human operator's (HO) visual references are relative to the moving ship deck rather than to inertial space, his spatial orientation with respect to the inertial space is impaired. Moreover, the helicopter is subjected to atmospheric disturbances that constitute a forcing function with a power density spectrum within the helicopter control bandwidth and that will thus require considerable pilot activity. This difficulty is enhanced by the fact that the landing area of small ships is small, and as a result, the hovering above the deck has to be carried out with great precision.

In a preliminary study of the present subject,[10] it has been shown that providing the pilot with explicit inertial position and rate information by means of display augmentation can reduce pilot workload and improve hovering performance. These results demonstrated the importance of displaying inertial position information, but the questions of how to realize this information and how to present the additional cues were not addressed.

Display augmentation can be implemented on the helicopter by means of a head-up display or a three-dimensional visual structure at the ship. With the measurement equipment typically available onboard a helicopter, it is very difficult to obtain accurate inertial position estimates in the cockpit. On the other hand, it is possible to estimate quite accurately the ship deck motion[8,9] and to use these estimates to generate ship-based, visual inertial references. Then the pilot, instead of deriving visual orientation cues from the moving ship deck,

Received Dec. 1, 1988; revision received July 21, 1989.

*Research Fellow, Faculty of Aerospace Engineering.
†Senior Lecturer, Faculty of Aerospace Engineering. Member AIAA.
‡Associate Professor, Faculty of Aerospace Engineering.

can derive cues from the inertially stable references, which are line-drawn, geometrical shapes. It was shown in Refs. 11–13 that the HO is able to derive his spatial orientation more accurately by viewing three-dimensional geometrical shapes, such as a box or cube, than by viewing two-dimensional flat images, such as a rectangle or square. Moreover, it was found in static viewing experiments[13] that the position judgment accuracy of a HO viewing a line-drawn image of a cube was independent of the azimuth and elevation angles of the observer's viewpoint with respect to the cube. Therefore, a line-drawn, inertially stable, cube structure was chosen as the ship-based visual reference, and it became of prime interest to investigate the inherent errors made by the pilot during the hovering task. The line-drawn cube can be created by a matrix of signal lights and can be stabilized using an electromechanical motion platform similar to the one described in Ref. 13. In spite of errors inherent in the estimation of the inertial position, in order to simplify the investigation it was assumed that the cube can be ideally stabilized.

There is a basic difference between the visual information presented to the pilot in the preliminary study[10] and the information in the present investigation. In the study of Ref. 10, position errors and their rates were presented explicitly. In contrast, with the use of the line-drawn cube, in the present study the HO has to estimate his position errors by internally processing the perspective shape of the cube. Moreover, additional difficulties arise from the unusual character of the longitudinal hovering dynamics. In the absence of substantial forward motion, pitching down of the noise of the helicopter will result in a forward surge motion, rather than a downward motion, like this is the case with fixed-wing aircraft. Thus, the fixed-wing aircraft pilot can link the pitch-down motion, as experienced by an upward shift of the horizon, to the rate of descent of the aircraft. For the hovering helicopter pilot this link does not exist and the vertical speed of the helicopter can be extracted only from changes in the perspective cube shape. However, the pitch motion as perceived through the vertical shift of the horizon, provides the pilot with surge rate and surge acceleration information.

This research includes analytical and experimental work. The analytical model of the hovering task is necessary for a better understanding of the effect of the various parameters on the task performance. Moreover, analytical and experimental results are mutually supporting in validating the hovering results and providing insight into the control mechanism.

Analytical models of man-machine systems are classified in the literature in two groups. The classical control engineering approach[14,15] indicates the state variables, which are required from a control theoretical point of view, without studying how these variables are perceived. The modern optimal control engineering approach[16–21] states that the well-trained, well-motivated HO behaves almost like an optimal controller subject to his inherent limitations and to the control task. In this model, the sources of HO remnant are specified as observation and motor noises. Observation noise accounts for uncertainty in the perception of parameters, whereas motor noise accounts for the random errors in executing the intended control movements. The optimal control model (OCM) is used both for instrument display control tasks[21–27] and visual field control tasks.[28–31]

In the present paper, the analytical and experimental results of the hovering task are presented. The visual field is augmented with a line-drawn cube as a ship-based reference, in combination with an artificial horizon provided on the helicopter head-up display. The cube is inertially stabilized above the ship and does not move with the ship's angular motions and heave. A simplified hovering task is considered in which helicopter motions exist in the longitudinal plane; the ship deck is subjected to heave motions only, without pitch or roll.

II. Analytical Model

The longitudinal hovering situation is described in Fig. 1. A general description of the display viewed by the pilot is given in Fig. 2. The pilot's task is to keep the helicopter at a desired inertial height, chosen such that a sudden collision between the ship and the helicopter will not occur. The task is performed in the presence of vertical atmospheric disturbances and vertical motions of the ship deck. The desired hovering altitude is presented to the pilot by means of a line-drawn cube. A horizontal bar that is attached to the ship's mast serves the pilot as a means to observe the motion of the helicopter, relative to the ship deck.

In the investigation, the surge (forward-backward) motion is assumed to be controlled by an autopilot. The helicopter pitch control is executed automatically by the automatic surge-control system, without intervention of the pilot. Thus, the pilot has to control the helicopter heave (vertical) motion only, using the collective lever. The atmospheric disturbances are assumed to influence only the helicopter vertical motion.

A. Dynamic Model

The dynamic model of the system consists of the linearized equations of motion of the helicopter, the equations representing the ship-deck motion, and the atmospheric disturbances. The equations of motion of the helicopter represent the motion in the vertical axis in response to the collective control input commands and the atmospheric disturbances. The atmospheric disturbances are modeled by a first-order Markov process. The ship-deck motion is modeled by a second-order Markov process. Summarizing the aforementioned assumptions, the dynamic model can be described by the following state equation:

$$\dot{x} = Ax + B\,\delta_c + w_d \qquad (1)$$

Equation (1) is elaborated on in the Appendix [see Eq. (A1)], and the state vector is defined as $x = \mathrm{col}(h, w, w_g, h_s, w_s)$.

The helicopter model used in the investigation represents a Bell UH-1H. The coefficients representing the helicopter in hovering flight at sea level were taken from Ref. 32.

B. Observation Model

The HO observations are relative to the inertial space and the moving ship deck. Therefore, according to the experimental conditions (to be described hereafter), the observation vector will include the absolute position and velocity, and/or

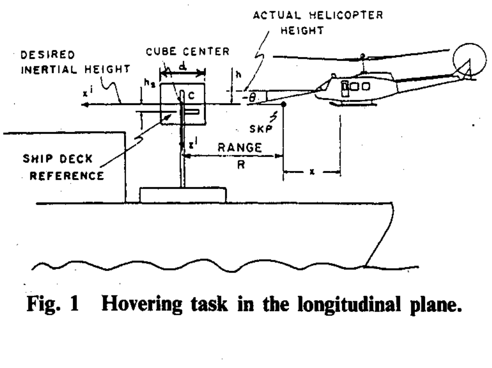

Fig. 1 Hovering task in the longitudinal plane.

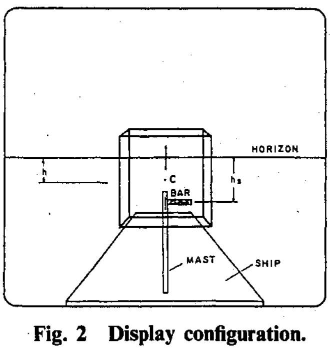

Fig. 2 Display configuration.

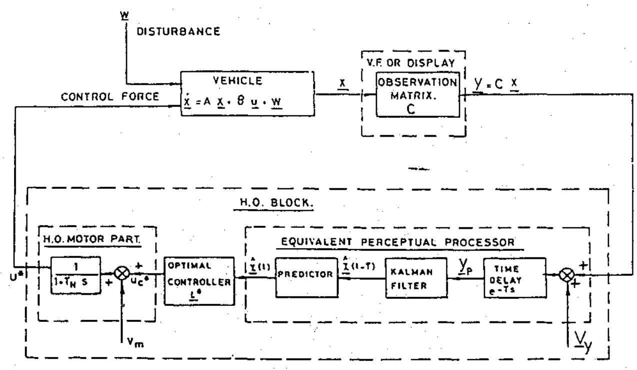

Fig. 3 Optimal control model.

the position and velocity relative to the deck. The observation vector can be described as a linear combination of the state vector by the following equation:

$$y(t) = Cx(t) + v_y(t) \tag{2}$$

The vector of observed variables, including the absolute and the relative position and velocity, is given by

$$y(t) = \mathrm{col}(h, w, h - h_s, w - w_s)$$

It is assumed[16] that the HO perceives observations that are delayed by τ s. Thus the noisy and delayed observation vector perceived by the HO $y_p(t)$ is given by

$$y_p(t) = Cx(t - \tau) + v_y(t - \tau) \tag{3}$$

C. Optimal Control Model

A block diagram of the OCM is shown in Fig. 3. The basic assumption of the OCM is that the HO has perfect knowledge of the vehicle and the measurement models. The HO action is accomplished in two stages:

1) Optimal reconstruction of the state variables from the noisy delayed vector of the observed variables. This is done by means of Kalman filtering and optimal prediction.

2) Determination of the control function δ_c^*, such that in the steady state the following cost function is minimized:

$$J(\delta_c) = \lim_{t_f \to \infty} E\left\{\frac{1}{t_f}\int_0^{t_f} [x^TQx + r\,\delta_c^2 + g\,\dot{\delta}_c^2]\,\mathrm{d}t\right\} \tag{4}$$

Q is the weighting matrix of x, and r and g are the weighting coefficients of δ_c and $\dot{\delta}_c$, respectively. Since the Kalman filter has a perfect knowledge of the optimal control δ_c^*, a perfect estimate of the state is obtained by simply integrating the state equations. On the other hand, it is clear that in reality the HO's estimates are not perfect. Therefore, to prevent the Kalman filter from perfectly knowing the control, a HO motor noise is added to the control force u_c^*, imparted to the neuromuscular system (see Fig. 3). This motor noise accounts for the fact that the HO does not know his control action precisely.

The inclusion of the control rate in the cost function is mathematically equivalent to the first-order neuromuscular dynamics in the transfer function of the HO.[16]

The solution of the reconstruction and control problem is derived from Kleinman et al.[16,18,21]

Several parameters of the analytical model are not known a priori. The unknown parameters can be determined by a model-matching procedure. This is a post-experimental procedure, in which the unknown parameters are adjusted such that the analytical model outputs, i.e., the covariances of state and control variables, match with their corresponding experimental values. The unknown parameters are as follows:

1) The weighting coefficients Q,r,g. Nevertheless, the elements of the diagonal matrix Q, which weight the uncontrollable but asymptotically stable state variables of the atmospheric disturbances and ship motion, can be a priori set to zero. Therefore, the unknown elements of Q are only the elements that weight the helicopter position and velocity, i.e., $Q = \mathrm{diag}(q_h, q_w, 0, 0, 0)$.

2) The time delay τ and the neuromuscular time constant τ_N.

3) The covariances of the observation noises V_y and motor noise V_m, which have been shown by Levinson et al.[20] to be proportional to the covariances of y and u_c, respectively. The noise levels at the observation and motor noises are defined as

$$V_{y_{i[\mathrm{db}]}} = 10 \log[V_{y_i}/\pi E\{y_i^2\}]$$

$$V_{m_{[\mathrm{db}]}} = 10 \log[V_m/\pi E\{u_c^2\}]$$

where i is the number of the measurement.

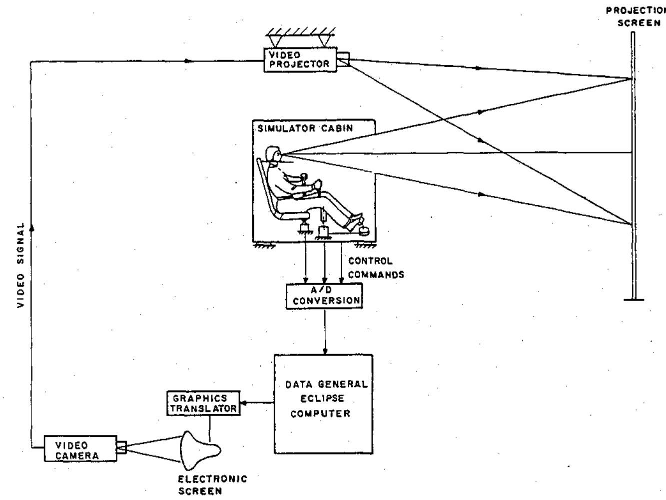

Fig. 4 Experimental setup.

III. Fixed Base Simulation Program

A. Experimental Setup

A block diagram of the fixed base simulation setup is shown in Fig. 4. The HO's control commands, translated into analog voltages, are converted to digital signals and are imparted to a digital simulation computer. The computer is programmed to solve the vehicle equations of motion and perform the necessary graphics calculations to create, in real time, the perspective image. This image, displayed on a cathode-ray tube (CRT) display, is received by a television camera and finally projected on a screen of 2.40 × 2.40 m placed 4.5 m in front of the subject. The projected image viewed by the subject is used to create the control commands that close the control loop.

B. Experimental Program

The experimental program started after a training period of four weeks. The four subjects who participated in the experimental program were undergraduate students of the Faculty of Aerospace Engineering and have participated as subjects in other aeronautical experimental programs in the past. The training period is especially important in view of the absence of motion cues, requiring the subjects to be familiarized with the image and with the motions of the ship and the helicopter. The subjects were instructed to keep the helicopter at a constant inertial height above the ship deck, using the collective control lever. The required height was referenced to the center of the cube and was not shown explicitly. The range of the SKP from the cube center was fixed at $R = 70$ ft and was kept constant throughout the experimental program. The effect of the cube size d was investigated. Three values of the ratio σ, which equals R/d, were investigated: $\sigma = 4$, 8, and 16.

The scope of the experimental program was as follows:

1) Investigation of how, and to what extent, the HO uses the various displayed visual cues. The question was whether explicit cues, such as the deviation of the horizon from the cube center, or implicit cues, such as the cues included in the perspective cube structure, are used.

2) Determination of the most effective display configuration for the given task.

3) Determination of the hovering accuracy in terms of the observed position errors for each display configuration.

During the investigation, nine experiments were conducted, which were divided into five series. For each experiment, each of the four subjects performed 5 runs, each of 168 s in duration. During each run, the time histories of the state and control variables were recorded by the computer.

1. Description of the Experiments

Series A: *Perspective visual cues only* (*Fig. 5*). Experiments 1, 2, and 3 were conducted to determine the HO's ability to perform the control task by deriving the position information from the perspective shape of the cube only. Therefore, in this series the visual scene included only the line-drawn cube. To insure that the perspective cube shape is the only visual cue, the helicopter longitudinal body axis x^b was pointed at all times at the center of the cube (the x^b axis was tethering about the cube center). Thus, the cube appeared always at the center of the screen. Experiments 1, 2, and 3 referred to values of $\sigma = 4$, 8, and 16, respectively.

Series B: *Perspective cues in the presence of pitch motion* (*Fig. 6*). In experiment 4, which was conducted at $\sigma = 8$, the ship image was displayed together with the perspective cube. The ship, which was subjected to heave motion, presented the pilot with references relative to the ship deck. The horizon line was not displayed and was assumed to be hidden by the ship's structure. In addition to the heave motion, the helicopter also executed a pitch motion, which was a result of the surge (forward-backward motion) autopilot activity and was not under the control of the pilot. Therefore, the pilot had to control only the helicopter heave motion. The helicopter pitch motion was simulated by a second-order Gaussian process, created by a white noise passed through a second-order filter with $\zeta = 0.1$ and $\omega = 0.5$ rad/s. This pitch motion caused the displayed image (ship and cube) to shift vertically on the screen, but the perspective shape of the image did not change. As a result, the pilot had to derive the positional information, as in series A, from the perspective shape of the cube. Because of the pitch activity, the uncorrelated vertical shift motions of the image on the screen acted, in this case, like a visual disturbance.

Series C: *Combination of perspective and explicit visual cues in the presence of pitch motion* (*Fig. 7*). Experiment 5 is similar to experiment 4, but in addition to the display of experiment 4, in experiment 5 the horizon line was also displayed. In this situation the HO has two sources from which the position error can be perceived. The first source is the perspective cube shape, as in the previous experiments. The second cue is the explicit heave error, perceived from the angular distance between the horizon line and the cube center. It should be noticed that the cube center, C was not displayed explicitly. The purpose of this experiment was to investigate if, and to what extent, the HO utilizes the explicit displacement information (in addition to the implicit information perceived from the cube shape).

Series D: *Combination of perspective and explicit visual cues without pitch motions* (*Fig. 8*). In experiments 6–8, the displayed scene included the ship, cube, and horizon. However, in this series, the helicopter did not execute pitch motion. Therefore, the horizon line appeared as a stationary horizontal line through the center of the screen. The purpose of these experiments was to investigate the mechanism of the explicit information perception, in the absence of the disturbing vertical shift of the displayed image, caused by the pitch motions. Experiments 6–8 were performed for $\sigma = 4$, 8, and 16, respectively.

Series E: *The baseline configuration* (*Fig. 9*). In experiment 9, the pilot's visual field was not augmented. In this baseline experiment, in which the helicopter did not execute pitch motion, only the ship and the horizon were displayed. The pilot did not perceive implicit nor explicit inertial position information. As presently executed, this experiment represents a highly simplified replica of the actual task. In this experiment, the subjects were instructed to maintain, as accurately as possible, the height given by the average position of the horizontal bar attached to the ship's mast. The purpose of this experiment was to investigate whether, and how accurately, the HO is able to perform the control task.

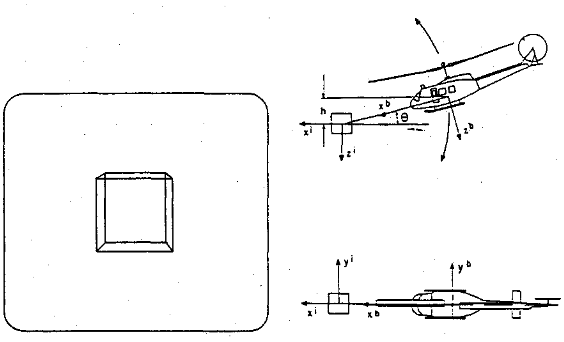

Fig. 5 Configuration of experiments 1–3.

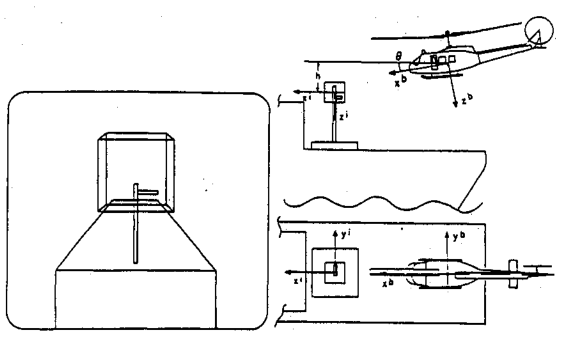

Fig. 6 Configuration of experiment 4.

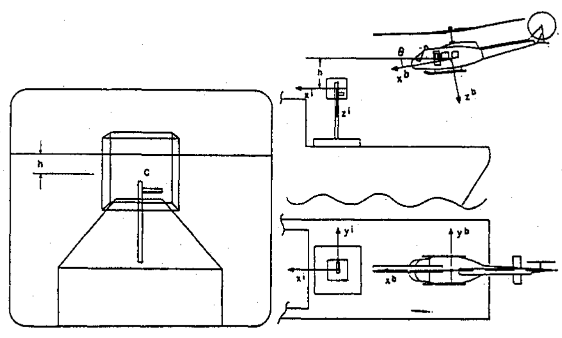

Fig. 7 Configuration of experiment 5.

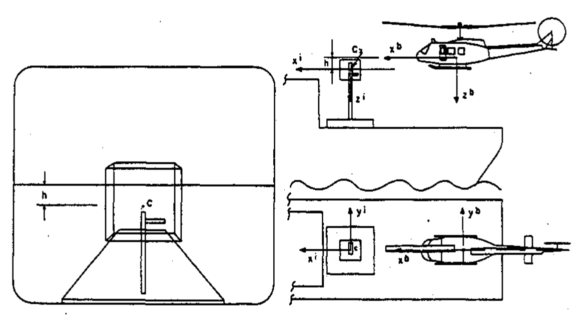

Fig. 8 Configuration of experiments 6–8.

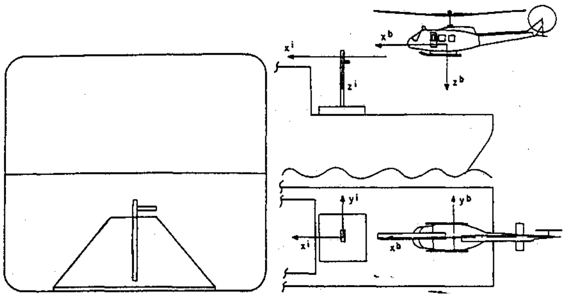

Fig. 9 Configuration of experiment 9.

The various experimental conditions are described in Table 1. The atmospheric disturbance was simulated by a first-order Markov process with $\text{cov}(w_g) = 20\ \text{ft}^2/\text{s}^2$ and a break frequency of 2 rad/s. The ship heave motion was simulated by a second-order Markov process with $\text{cov}(h_s) = 6\ \text{ft}^2$, approximating sea state five.

2. Experimental Results

Post experimental processing included the computation of the means and the covariances of the time histories of the state and control variables for each run and for each subject. The results presented in Table 2 are the averaged covariances over all subjects and all trial runs. They represent the mean and the standard deviation of the covariances of the helicopter position and velocity and the control activity. The averaged means of the time histories were very close to zero. In addition to the results presented in Table 2, Figs. 10–15 depict the time histories of the altitude and the control activity of a typical run for each one of the nine experiments. Table 2 also presents the results of the analytical model after they had been matched to the experimental data. In this procedure, the model's unknown parameters, i.e., q_h, q_w, r, g, V_{y_i}, V_m, τ, and τ_N were adjusted such that the covariances of h, w, and δ_c were matched with their corresponding experimental values. The parameters yielding the "best match" are listed in Table 3. In general, the following can be concluded:

1) A very good match is established between the analytical and the experimental results.

2) For all the experiments, the following best match values were obtained: time constant $\tau = 0.1$ s, neuromuscular time constant $\tau_N = 0.2$ s, motor noise levels about -20 dB. These values are typical for manual control tasks.[10,21–24,27–31]

Results of series A. In Figs. 10–12 the effect of σ, the cube size-to-range ratio, is demonstrated. It can be seen that, for $\sigma = 4$, because of the large cube image (Fig. 10), the height errors are relatively small. The stick activity shows the existence of high-frequency components, probably resulting from an increased HO gain in the feedback loop. For $\sigma = 8$, the cube image becomes smaller and consequently it becomes more difficult for the HO to estimate his height. Therefore, Fig. 11 shows the existence of periods during which the HO does not change the control input. Such a period lasts until the HO succeeds in estimating his height. As a result, the

Table 1 Experimental conditions

Experiment	Display Configuration				Comments
	Ship	Horizon	Cube	$\sigma = R/d$	
1	−	−	+	4	
2	−	−	+	8	
3	−	−	+	16	
4	+	−	+	8	Pitch motion present
5	+	+	+	8	Pitch motion present
6	+	+	+	4	
7	+	+	+	8	
8	+	+	+	16	
9	+	+	−	8	

(+) Displayed; (−) not displayed

Table 2 Comparison between the model and experimental results

Experiment	cov(h), ft²		cov(w), ft²/s²		cov(δ_c), in.²	
	Experiment	Model	Experiment	Model	Experiment	Model
1	2.09 ±0.26	2.29	3.92 ±0.66	2.75	0.155 ±0.038	0.127
2	6.08 ±1.71	6.96	5.31 ±1.35	4.14	0.113 ±0.041	0.123
3	14.90 ±2.83	12.40	8.49 ±2.34	6.08	0.136 ±0.066	0.191
4	4.73 ±1.08	4.59	3.91 ±0.68	3.46	0.101 ±0.052	0.134
5	1.29 ±0.42	1.17	2.27 ±0.55	1.85	0.123 ±0.041	0.101
6	0.80 ±0.23	1.04	2.06 ±0.39	1.72	0.138 ±0.025	0.096
7	1.10 ±0.32	1.04	2.06 ±0.67	1.72	0.104 ±0.029	0.096
8	1.11 ±0.24	1.04	2.16 ±0.55	1.72	0.110 ±0.030	0.096
9	9.67 ±2.71	—	7.01 ±1.88	—	0.133 ±0.033	—

Table 3 Matched parameters of the analytical model

Experiment	Measurement model	V_y, dB	cov y	V_y	q_h/g	q_w/g	r/g	V_m, dB
1	$y_1 = h$	-18	2.29	0.102	1.22	0.51	3.1	-18
	$y_2 = w$	-6	2.17	0.013		$g = 9.76$		
2	$y_1 = h$	-7	6.96	3.83	1.22	0.51	3.1	-24
	$y_2 = w$	-5	4.14	1.08		$g = 9.76$		
3	$y_1 = h$	-5	12.4	12.3	1.22	0.51	3.1	-22
	$y_2 = w$	-5	6.08	6.01		$g = 9.76$		
4	$y_1 = h$	-6	4.59	3.62				
	$y_2 = w$	-4	3.46	4.33	1.22	0.51	3.1	-20
	$y_3 = h - h_s$	-11	8.87	2.21		$g = 9.76$		
	$y_4 = w - w_s$	-11	6.28	1.56				
5	$y_1 = h$	-13	1.17	0.18				
	$y_2 = w$	-12	1.85	0.36	2.11	0.07	3.5	-20
	$y_3 = h - h_s$	-11	7.24	1.81		$g = 7.09$		
	$y_4 = w - w_s$	-11	5.74	1.43				
6, 7, 8	$y_1 = h$	-14	1.04	0.13				
	$y_2 = w$	-12	1.72	0.34	2.11	0.07	3.5	-20
	$y_3 = h - h_s$	-11	7.30	1.82		$g = 7.09$		
	$y_4 = w - w_s$	-11	5.10	1.27				

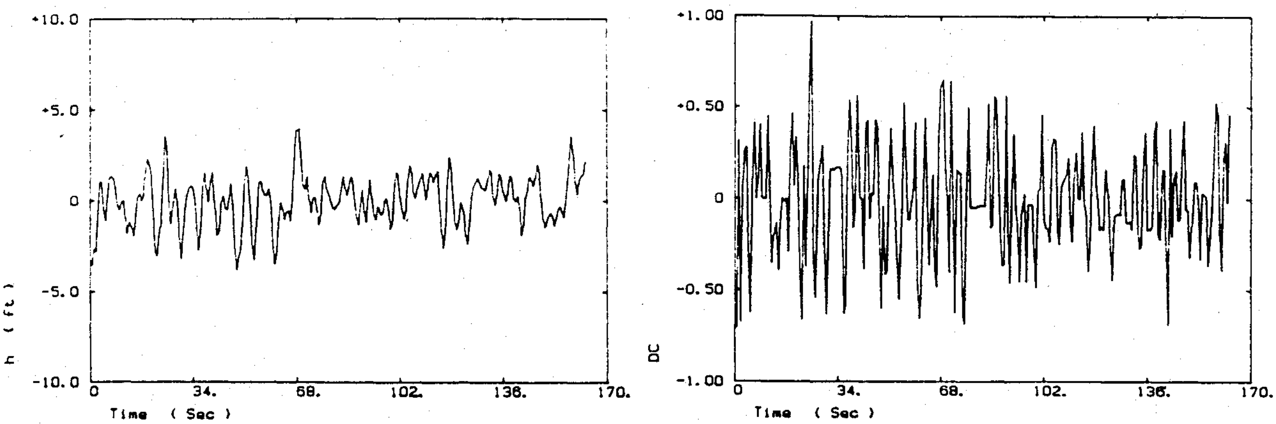

Fig. 10 Time histories of h and δ_c of experiment 1.

height errors are higher for $\sigma = 8$ than for $\sigma = 4$. The same characteristics, but to a greater degree, can be seen in Fig. 12, depicting the results of experiment 3 in which $\sigma = 16$.

The analytical model included observations of the inertial position and velocity of the helicopter. It can be seen in Table 3 that the position observation noise level increases with σ. In experiment 1 the observation noise covariance $V_h = 0.102\ \mathrm{ft}^2$ is about 5% of the covariance of the measured variable $\mathrm{cov}(h) = 2.29\ \mathrm{ft}^2$. In experiment 3, V_h and $\mathrm{cov}(h)$ are almost equal. Therefore, it can be concluded that satisfactory estimation is obtained only for relatively large cube sizes or, alternatively, if the cube is viewed from a short range. Both of these situations are not practical because of the small ship dimensions and the required rotor clearance.

Results of series B and C. The results of experiment 4 are presented in Fig. 13. These results are quite similar to the results of experiment 2, which was conducted with $\sigma = 8$ as well. The covariances of h, w, and δ_c are also very similar (Table 2) in both experiments. This similarity was expected because in both experiments the visual cues used during the HO's spatial orientation process were derived from the perspective shape of the cube only. It was also expected that the disturbing vertical shifts caused by the pitch motions would somewhat degrade the performance. Nevertheless, it can be seen in Table 2 that the covariances of h, w, and δ_c in experiment 4 are about the same (and even smaller) than the ones obtained with the cues in experiment 2. Comparison between Figs. 10 and 12 shows quite similar behavior in both experiments. This means that the pitch motion did not affect the ability of the subjects to derive implicit positional information from the cube structure.

The results of experiment 5 are depicted in Fig. 14. Comparison between the results of experiments 4 and 5 shows that the additional explicit information presented in experiment 5 markedly improves the hovering performance. This improvement includes approximately 75% reduction of the height error covariance, 50% reduction of the velocity covariance, and 20% reduction of the control activity (see Table 2).

The observation vector of the analytical model, for both the B and C series, included inertial and deck-relative observations. The noise levels for the absolute position and velocity were found to be -6 and -4 dB in experiment 4, and -13 and -12 dB in experiment 5. This indicates that the inertial observations are much more accurate when the explicit information is presented. The noise levels relative to the deck observations were found to be -11 dB in both experiments.

Results of series D. The results of experiments 6–8, tabulated in Table 2, show a great deal of similarity, in spite of the fact that the cube image becomes smaller with increasing σ. It was shown in the results of series A that for the smallest apparent cube size ($\sigma = 16$) the ability to derive positional information from the cube shape is highly impaired. But in experiment 8, the hovering performance is almost similar to the performance shown in experiments 6 and 7. Therefore, it can be concluded that the HO uses the explicit information for his inertial measurements rather than the cues perceived from the perspective cube shape. Comparison between the results of the experiments of series D, with the results of series

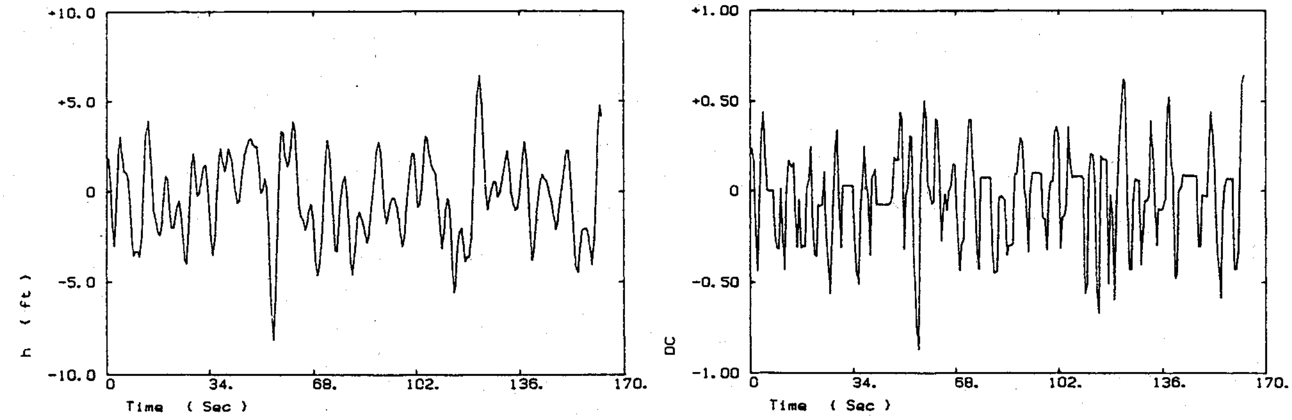

Fig. 11 Time histories of h and δ_c of experiment 2.

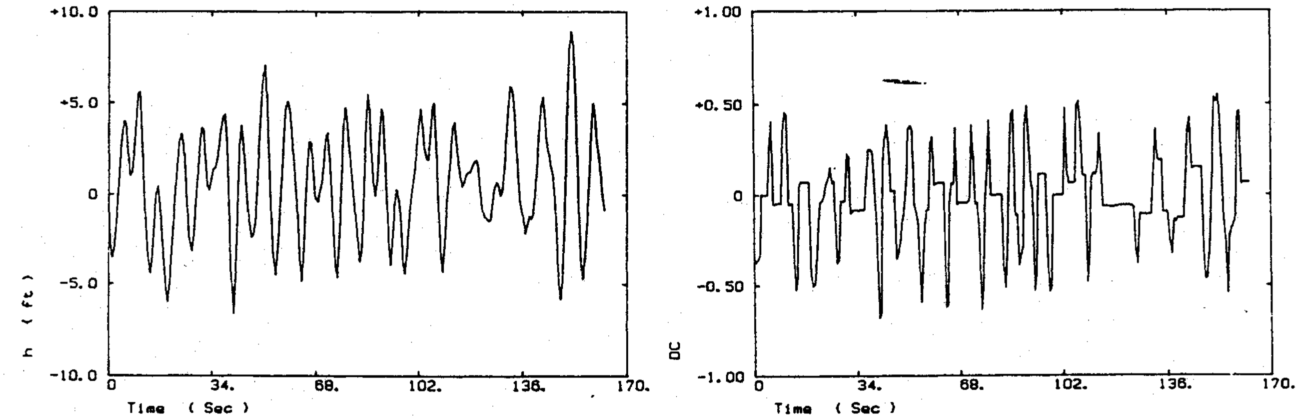

Fig. 12 Time histories of h and δ_c of experiment 3.

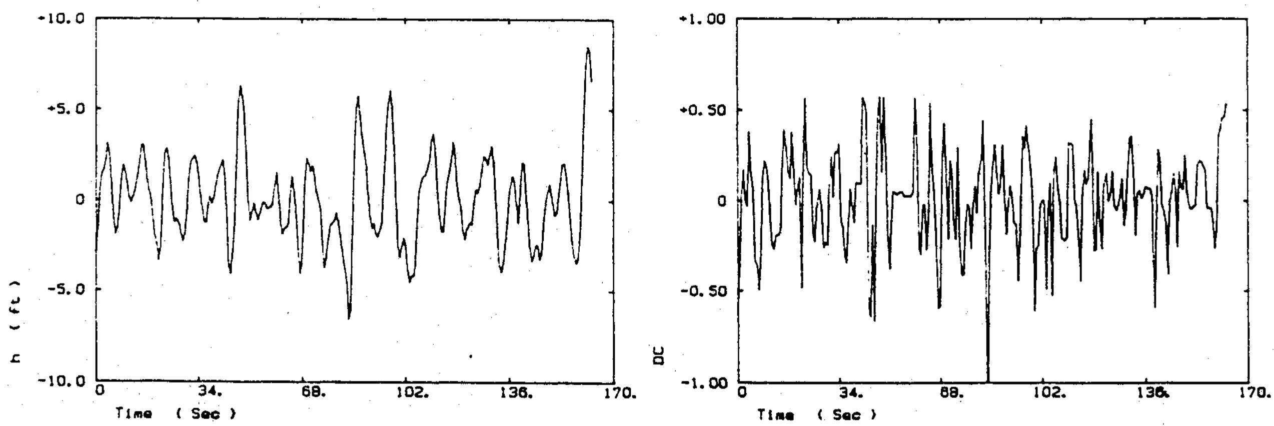

Fig. 13 Time histories of h and δ_c of experiment 4.

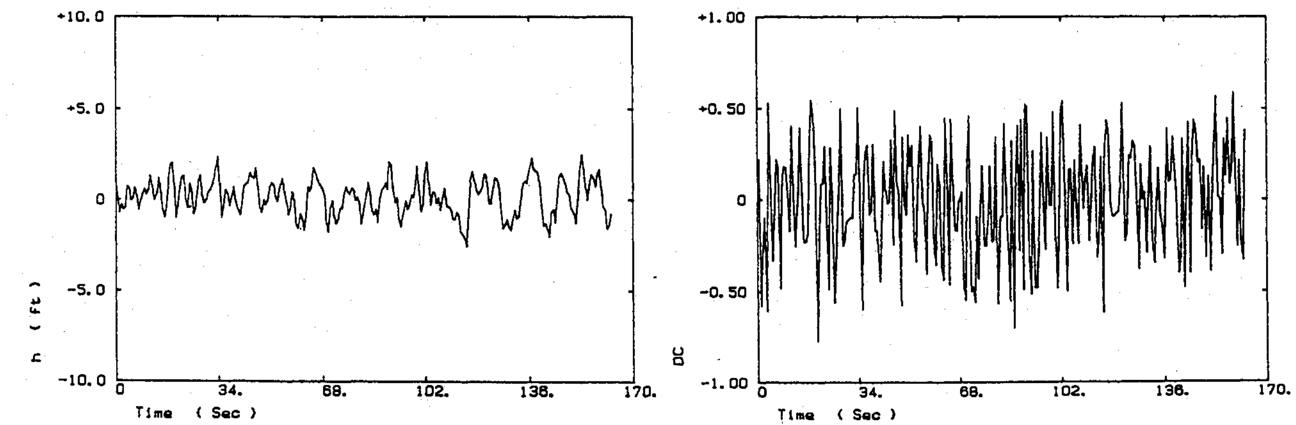

Fig. 14 Time histories of h and δ_c of experiment 5.

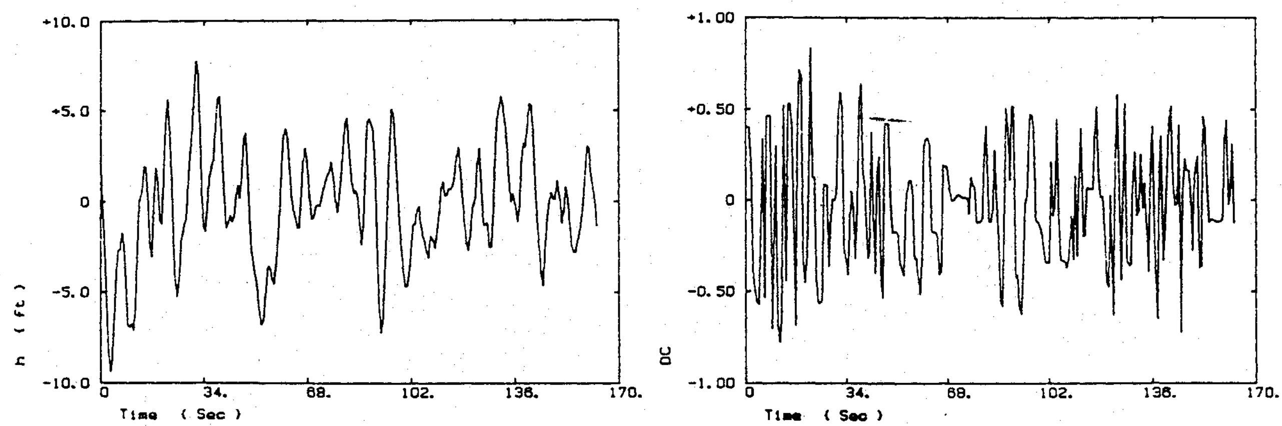

Fig. 15 Time histories of h and δ_c of experiment 6.

C, indicates that the disturbing pitch motions do not affect the performance. The reason is that the vertical shift of the image, in series C, does not affect the angular distance between the horizon and the cube center and, thus, does not affect the explicit positional cues.

Since the experimental results of the three experiments in series D yielded similar covariances, only one set of parameters was sought in the model-matching procedure. Similar to experiment 5, the observation vector in experiments 6–8 included inertial and deck-relative observations. The analytical results in this case were found to be similar to the analytical results of the C series.

Results of Series E. The results of experiment 9 in which the pilot's visual field was not augmented are shown in Fig. 15. It can be seen that there exist relatively long periods of time in which the HO did not change the collective control setting. Following these periods of inactivity, large control commands were applied, which resulted in large height errors. Moreover, in this experiment, a strong tendency of the subjects to track the deck motion was noticed (although they were instructed to avoid tracking it). Therefore, all the three covariances in this experiment are among the highest of all the experiments.

For this experiment, it is not possible to match an analytical model in the optimal control model framework. The reason is that the analytical model requires full observability of the state vector. In experiment 9 the observations are relative to the ship deck only. Therefore, the inertial height and velocity necessary to close the control loop are unobservable. Nevertheless, the subjects succeeded in performing the hovering task, to some extent, because the ship motion forcing function was bounded.

IV. Conclusions

The display of inertial position information can be effectively utilized by the pilot. Consequently, the performance of the helicopter hovering task above a moving ship deck is markedly improved.

Implicit information concerning the inertial position of the helicopter can be realized by creating a line-drawn, inertially stable cube above the ship deck. This information is effective only for relatively large cube sizes, or alternatively for a cube viewed from a short range. Both situations are impractical for a helicopter landing on a small ship deck because of the ship dimensions and the required rotor clearance.

Explicit inertial position information of the helicopter can be created by combining the line-drawn cube implemented above the ship deck with a horizon bar displayed on the helicopter head-up display.

The human operator uses the explicit positional information rather than the implicit information perceived from the perspective shape of the line-drawn cube. The horizon bar, presented on the head-up display, in combination with an inertially stable, ship-based cube structure of relatively small dimensions, is therefore a successful combination for providing the inertial position information in the vertical hovering task.

The optimal control model is used as a mathematical framework for studying the hovering task. Using the analytical model, the observation and motor noises, the inherent human limitations, and the system performance are modeled. Comparison of the analytical results with experimental results provides a useful framework for studying these human characteristics.

Appendix: State Equation and Observation Matrices of the Analytical Model

The state equations representing the various experimental conditions are

For Experiments 1–3

$$\dot{x} = \begin{bmatrix} \dot{h} \\ w \\ w_g \end{bmatrix} = \begin{bmatrix} 0 & 1 & 0 \\ 0 & z_w & z_w \\ 0 & 0 & -a \end{bmatrix} \begin{bmatrix} h \\ w \\ w_g \end{bmatrix} + \begin{bmatrix} 0 \\ z_{\delta_c} \\ 0 \end{bmatrix} \delta_c + \begin{bmatrix} 0 \\ 0 \\ a \end{bmatrix} n_g \tag{A1}$$

For Experiments 4–9

$$\dot{x} = \begin{bmatrix} \dot{h} \\ w \\ w_g \\ h_s \\ w_s \end{bmatrix} = \begin{bmatrix} 0 & 1 & 0 & 0 & 0 \\ 0 & z_w & z_w & 0 & 0 \\ 0 & 0 & -a & 0 & 0 \\ 0 & 0 & 0 & 1 & 0 \\ 0 & 0 & 0 & -\omega_s^2 & -2\xi_s\omega_s \end{bmatrix} + \begin{bmatrix} h \\ w \\ w_g \\ h_s \\ w_s \end{bmatrix}$$

$$+ \begin{bmatrix} 0 \\ z_{\delta_c} \\ 0 \\ 0 \\ 0 \end{bmatrix} \delta_c + \begin{bmatrix} 0 & 0 \\ 0 & 0 \\ a & 0 \\ 0 & 0 \\ 0 & \omega_s^2 \end{bmatrix} \begin{bmatrix} n_g \\ n_s \end{bmatrix} \tag{A2}$$

where n_g and n_s are zero-mean Gaussian white noise processes

$$z_w = 0.385\ \mathrm{s}^{-1}, \qquad z_{\delta_c} = -9.77\ (\mathrm{ft/s^2})/\mathrm{in.},$$

$$a = 2\ \mathrm{s}^{-1}, \qquad \omega_s = 0.8\ \mathrm{rad/s}, \qquad \xi = 0.05$$

The observation matrices are

For Experiments 1–3:

$$C = \begin{bmatrix} 1 & 0 & 0 \\ 0 & 1 & 0 \end{bmatrix} \tag{A3}$$

For Experiments 4–8:

$$C = \begin{bmatrix} 1 & 0 & 0 & 0 & 0 \\ 0 & 1 & 0 & 0 & 0 \\ 1 & 0 & 0 & -1 & 0 \\ 0 & 1 & 0 & 0 & -1 \end{bmatrix} \tag{A4}$$

References

[1]"Operation of Naval Helicopters from Small Ships," Westland Helicopters, Ltd., Yeovil, England, U.K.

[2]Tuttle, R. M., "A Study of Helicopter Landing Behavior on Small Ships," *Journal of the American Helicopter Society*, Vol. 21, 1976, pp. 2–11.

[3]Bryson, L. B., Heenan, F. E., and Johnson, C. A., "Helicopters in the Royal Navy," *Aeronautical Journal*, Vol. 76, 1972, pp. 469–500.

[4]Beck, D. E., "USN, Navy Shipboard Trials of Helicopters and V/STOL Aircraft," *Journal of the American Helicopter Society*, Vol. 21, 1976, pp. 2–11.

[5]Carico, D., McCallum, K. E., and Higman, J., "Dynamic Interface Flight Test and Simulation Limitations," 11th European Rotorcraft Forum, London, Sept. 1985.

[6]Merrick, V. K., and Gerdes, R. M., "VTOL Controls for Shipboard Operations," *Overview of the JVX-Program SP-555 Powered Lift Systems Plus*, Aerospace Congress and Exposition, Long Beach, CA, Oct. 1983.

[7]Paulk, C. H., Jr., Donley, S. T., and Hollis, M. K., "Evaluation of Control and Display Configurations for Helicopter Shipboard Operations," AIAA Paper 83-2486, Oct. 1983.

[8]McGee, L. A., Schmidt, S. F., and Miyashiro, S. K., "Navigation Performance of the TRISCAN Concept for Shipboard VTOL Aircraft Operations," AIAA Paper 78-1293, 1978.

[9]McGee, L. A., Paulk, C. H., Jr., Steck, S. A., Schmidt, S. F., and Merz, A. W., "Evaluation of Navigation Performance of Shipboard VTOL Landing Guidance Systems," *Journal of Guidance, Control, and Dynamics*, Vol. 4, 1981, pp. 433–440.

[10]Negrin, M., Grunwald, A., and Rosen, A., "Preliminary Study of Man-Machine Problems in Hovering Above a Moving Platform," *Vertica*, Vol. 9, 1985, pp. 51–64.

[11]Negrin, M., and Grunwald, A., "A Model for Human Spatial Orientation Using Familiar Object Cues," 27th Israel Annual Conference on Aviation and Astronautics, Feb. 1985.

[12]Grunwald, A., and Negrin, M., "A Model for Human Spatial Orientation Using Familiar Object Cues," *Human Decision Making and Manual Control*, edited by H. P. Willumeit, Elsevier Science, North Holland, 1986.

[13]Negrin, M., "Investigation of Man-Machine Problems in Helicopter Hovering Above a Moving Platform," DSc Thesis, Technion—Israel Institute of Technology, April 1987 (in Hebrew).

[14]McRuer, D. T., and Krendel, E. S., "Mathematical Models of Human Pilot Behavior," Systems Technology, Inc., Hawthorne, CA, AGARDograph 188, Jan. 1974.

[15]Weir, D. H., and McRuer, D. T., "A Theory for Driver Steering Control of Motor Vehicles," Systems Technology, Inc., Hawthorne, CA, preprint from Highway Research, Record 247, 1968.

[16]Kleinman, D. L., Baron, S., and Levinson, W. H., "An Optimal Control Model of Human Response, Part I: Theory and Validation," *Automatica*, Vol. 6, 1970, pp. 357–370.

[17]Kleinman, D. L., Baron, S., and Levinson, W. H., "An Optimal Control Model of Human Response, Part II: Prediction of Human Performance in a Complex Task," *Automatica*, Vol. 6, 1970, pp. 371–383.

[18]Baron, S., and Kleinman, D. L., "The Human as an Optimal Controller and Information Processor," *IEEE Transactions on Man-Machine Systems*, Vol. 10, 1969, pp. 9–17.

[19]Kleinman, D. L., "Optimal Control of Linear Systems with Time Delay and Observation Noise," *IEEE Transactions on Automatic Control*, Vol. 10, Inst. of Electrical and Electronics Engineers, Piscataway, NJ, 1969, pp. 524-527.

[20]Levinson, W. H., Baron, S., and Kleinman, D. L., "A Model of Human Controller Remnant," *IEEE Transactions on Man-Machine Systems*, Vol. MMS-10, 1969, pp. 101–108.

[21]Baron, S., Kleinman, D. L., Miller, D. C., Levinson, W. H., and Elkind, J. I., "Applications of Optimal Control Theory to the Prediction of Human Performance in a Complex Task," Wright-Patterson AFB, OH, AFFDL-TR-60-81, March 1970.

[22]Wewerinke, P. H., "Effort Involved in Single and Two-Axis Manual Control Systems," National Aerospace Laboratory, The Netherlands, NLR-TR-75060U, June 1975.

[23]Wewerinke, P. H., "Mathematical Models of Manned Aerospace Systems," National Aerospace Laboratory, The Netherlands, NRL-MP-78019U, July 1978.

[24]Wewerinke, P. H., "Mathematical Models of Pilot-Helicopter Systems," National Aerospace Laboratory, The Netherlands, NLR-MP-79026U, June 1979.

[25]Hess, R. A., and Wheat, L. W., "A Model-Based Analysis of a Display for Helicopter Landing Approach," *IEEE Transactions on SMC*, Vol. 7, Inst. of Electrical and Electronics Engineers, Piscataway, NJ, 1976, pp. 505–511.

[26]Hess, R. A., "Application of a Model-Based Flight Director Design Technique to a Longitudinal Hover Task," *Journal of Aircraft*, Vol. 14, 1977, pp. 265–271.

[27]Johannsen, G., and Govindaraj, T., "Analysis of a VTOL Hover Task with Predictor Displays, Using an Optimal Control Model of the Human Operator," 14th Annual Conference of Manual Control, April 1978, pp. 237–251.

[28]Grunwald, A., and Merhav, S. J., "Vehicular Control by Visual Field Cues—Analytical Model and Experimental Validation," *Transactions on SMC*, Vol. 6, Inst. of Electrical and Electronics Engineers, Piscataway, NJ, 1976, pp. 835–845.

[29]Wewerinke, P. H., "Visual Scene Perception Process Involved in the Manual Approach," National Aerospace Laboratory, The Netherlands, NLR-TR-78130U, May 1978.

[30]Wewerinke, P. H., "Visual Scene Perception—Frequency Domain Data and Model Parameter Estimation Procedure," National Aerospace Laboratory, The Netherlands, NLR-MP-79009U, March 1979.

[31]Wewerinke, P. H., "The Effect of Visual Information on the Manual Approach and Landing," National Aerospace Laboratory, The Netherlands, NLR-TR-80055U, May 1980.

[32]Heffley, R. K., and Jewell, W. F., "A Compilation and Analysis of Helicopter Handling Qualities Data," Vol. 1: Data Compilation NASA CR-3144, and Vol. 2: Data Analysis, NASA CR-3145, 1979.